Novel constraints on fermionic dark matter from galactic observables I: The Milky Way

C. R. Argüelles[a,b], A. Krut[b,c,d], J. A. Rueda[b,c,e], R. Ruffini[b,c,e]

[a] *Instituto de Astrofísica de La Plata (CCT La Plata, CONICET, UNLP), Paseo del Bosque, B1900FWA La Plata, Argentina*
[b] *ICRANet, Piazza della Repubblica 10, I–65122 Pescara, Italy*
[c] *Dipartimento di Fisica and ICRA, Sapienza Università di Roma, P.le Aldo Moro 5, I–00185 Rome, Italy*
[d] *University of Nice-Sophia Antipolis, 28 Av. de Valrose, 06103 Nice Cedex 2, France*
[e] *ICRANet-Rio, CBPF, Rua Dr. Xavier Sigaud 150, Rio de Janeiro, RJ, 22290–180, Brazil*

Abstract

We have recently introduced a new model for the distribution of dark matter (DM) in galaxies based on a self-gravitating system of massive fermions at finite temperatures, the Ruffini-Argüelles-Rueda (RAR) model. We show that this model, for fermion masses in the keV range, explains the DM halo of the Galaxy and predicts the existence of a denser quantum core at the center. We demonstrate here that the introduction of a cutoff in the fermion phase-space distribution, necessary to account for the finite Galaxy size, defines a new solution with a central core which represents an alternative to the black hole (BH) scenario for SgrA*. For a fermion mass in the range $mc^2 = 48 - 345$ keV, the DM halo distribution is in agreement with the Milky Way rotation curve data, while harbors a dense quantum core of about $4\times10^6 M_\odot$ within the S2-star pericenter.

Keywords: Methods: numerical – Cosmology: dark matter – Galaxies: halos, nuclei, structure

1. Introduction

The problem of the distribution of stars in globular clusters, and more general in galactic systems, has implied one of the results of most profound interest in classical astronomy. In particular, in the pioneering works of Michie (1963) and King (1966), they considered the effects of collisional relaxation and tidal cutoff by studying solutions of the Fokker-Planck equation. There, it was shown that stationary solutions exist and are well described by isothermal spheres models, based on simple Maxwellian energy distributions with a constant subtracting term interpreted as an energy cutoff. An extension of this statistical analysis with thermodynamic considerations, which includes the effects of violent (collisionless) relaxation, has been studied in Lynden-Bell (1967), with implications to the problem of virialization in galaxies which are still of current interest (see e.g. Binney and Tremaine, 2008).

Following the work of Ruffini and Bonazzola (1969) the attention has been directed to the possible role of quantum statistics as opposed to the Boltzmannian description. Attention has correspondingly shifted from stars to elementary particles. There the case of bosons as well as fermions was considered. This also shifted the interest from the baryonic matter composing a star to a new field of interest, which has become since of great relevance, the dark matter (DM) components of galactic structures.

A first significant attempt was made by Baldeschi et al. (1983) who called attention on the possible role of self-gravitating bosons for explaining galactic halos. Their result suggested as a viable DM candidate low particle masses down to 10^{-24} eV. This idea was further developed by a large number of authors. For a recent review of the initial work as well as the large number of intervening works see e.g. Hui et al. (2017), and references therein.

While the works on bosons were addressing the possible smallest particle mass in nature an alternative line of research of self-gravitating fermions of masses larger than few keV, also indicated by Baldeschi et al. (1983), addresses the system of semi-degenerate self-gravitating fermions with the aim of describing galactic DM halos (see e.g. Gao et al., 1990). Further, it was considered a quantum fermionic distribution taking into account the possible presence of a cutoff in the energy as well as in the angular momentum (Ruffini and Stella, 1983; Merafina and Ruffini, 1989; Ingrosso et al., 1992). A remarkable contribution in the understanding of these issues was given in Chavanis (2004), based on the study of generalized kinetic theories accounting for collisionless relaxation processes, and leading to a class of generalized Fokker-Planck equation for fermions. It was there explicitly shown the possibility to obtain, out of general thermodynamic principles, a generalized Fermi-Dirac distribution function including an en-

Email addresses: carlos.arguelles@icranet.org (C. R. Argüelles), andreas.krut@icranet.org (A. Krut), jorge.rueda@icra.it (J. A. Rueda), ruffini@icra.it (R. Ruffini)

ergy cutoff, extending the former Boltzmannian results by Michie (1963) and King (1966) to quantum particles.

More recently, it was shown that quantum particles fulfilling fermionic quantum statistics and gravitational interactions are able to successfully describe the distribution of galactic DM halos when compared with observations (Argüelles et al., 2013; de Vega et al., 2014; Argüelles et al., 2014a; Siutsou et al., 2015; Ruffini et al., 2015). A similar approach to galactic halos has been developed in Chavanis et al. (2015) within the so-called fermionic King model, but lacking information on the fermion mass and of general relativistic effects which become important for the quantum cores approaching the critical mass for gravitational collapse. In particular, Ruffini et al. (2015) proposed a new model (hereafter RAR model) addressing the simultaneous fulfillment of the dense quantum core to the classical halo distribution. There the RAR model was proposed as a viable possibility to establish a link between the dark central cores to DM halos within a unified approach.

In this paper we extend the RAR model by introducing a cutoff in the momentum distribution to account for (1) finite galaxy sizes (analogously as previously done in Ingrosso et al., 1992), and (2) to account for more realistic galaxy relaxation mechanisms as indicated above and in Chavanis (2004); providing a new family of solutions with an overall re-distribution of the bounded fermions.

Consequently, the more stringent outer halo constraints of our novel configurations allow a higher compactness of the central cores. In fact, the possibility of a fermion core at the Galactic center as an alternative to the central BH, first studied in Bilic et al. (2002) in the framework of Newtonian gravity, did not succeed in reaching the correct compactness of the quantum core since the cutoff energy parameter was not there considered.

Thus, the key questions to be answered here are the following:

- can the gravitational potential of the new quantum core sited at the center of the DM halo be responsible for the observed dynamics of the surrounding gas and stars, without the necessity of introducing a central BH?
- if so, which is the allowed DM fermion mass range to account for such observational constraints?

We answer here the above questions by making a detailed analysis of the theoretical RAR DM profiles. We present in section 2 the details of the general relativistic equilibrium equations of this model and discuss the general features of the physical variables. Then, by using a recent and extensive observational study of the Milky Way rotation curves (Sofue, 2013), and including the central S-star cluster data (Gillessen et al., 2009), we show here (see section 3) for the first time:

1. That a regular and continuous distribution of keV fermions can be an alternative to the BH scenario in SgrA*, being at the same time in agreement with the Milky Way DM halo, and without spoiling the known baryonic (bulge and disk) components which dominate at intermediate scales.
2. By constraining the DM quantum core to have the minimum compactness required by the S2 star dynamics, and by requesting the gravitational stability of the entire DM configuration, the fermion mass can be constrained to the range $mc^2 = 48 - 345$ keV.

Finally in section 4 we provide a discussion of the main results of our work, and further comment on where it stands with respect to the current affairs of cosmological DM and structure formation, indicating its potentiality to solve some of the actual discrepancies within the standard ΛCDM and ΛWDM cosmologies.

2. The Ruffini-Argüelles-Rueda (RAR) model

Following Ingrosso et al. (1992); Ruffini et al. (2013), we consider a system of self-gravitating massive fermions with a cutoff in the phase-space distribution under the assumption of thermodynamic equilibrium in general relativity.

A quantum phase-space function of this kind can be obtained as a (quasi) stationary solution of a generalized Fokker-Planck equation for fermions including the physics of violent relaxation and evaporation, appropriate to treat non-linear galactic DM halo structure formation (Chavanis, 2004). These phase-space solutions fulfill a maximization (Fermi-Dirac) entropy principle at fixed DM halo mass (bounded in radius) and temperature, consistent with the solutions given here, and further justifying the above assumed thermodynamic equilibrium approximation.

The fermionic equation of state can be written by

$$\rho = m\frac{2}{h^3}\int_0^{\epsilon_c} f_c(p)\left(1+\frac{\epsilon(p)}{mc^2}\right)d^3p\,, \tag{1}$$

$$P = \frac{1}{3}\frac{2}{h^3}\int_0^{\epsilon_c} f_c(p)\,\epsilon\,\frac{1+\epsilon(p)/2mc^2}{1+\epsilon(p)/mc^2}d^3p\,, \tag{2}$$

where the integration is carried out over the momentum space bounded from above by $\epsilon \leq \epsilon_c$, with ϵ_c the cutoff energy (see below); $f_c(p)$ is the phase-space distribution function differing from the standard Fermi-Dirac in the energy cutoff as

$$f_c(\epsilon \leq \epsilon_c) = \frac{1-e^{(\epsilon-\epsilon_c)/kT}}{e^{(\epsilon-\mu)/kT}+1}, \qquad f_c(\epsilon > \epsilon_c) = 0\,, \tag{3}$$

where $\epsilon = \sqrt{c^2p^2+m^2c^4}-mc^2$ is the particle kinetic energy, μ is the chemical potential with the particle rest-energy subtracted off, T is the temperature, k is the Boltzmann constant, h is the Planck constant, c is the speed of light, and m is the fermion mass. We do not include the presence of anti-fermions, i.e. we consider temperatures $T \ll mc^2/k$. The full set of (functional) parameters of the model are

defined by the temperature, degeneracy and cutoff parameters, $\beta = kT/(mc^2)$, $\theta = \mu/(kT)$ and $W = \epsilon_c/(kT)$, respectively.

We consider the system as spherically symmetric so we adopt the metric

$$ds^2 = e^{\nu}c^2dt^2 - e^{\lambda}dr^2 - r^2d\Theta^2 - r^2\sin^2\Theta d\phi^2, \quad (4)$$

where (r,Θ,ϕ) are the spherical coordinates, and ν and λ depend only on the radial coordinate r.

The thermodynamic equilibrium conditions are (Tolman, 1930; Klein, 1949):

$$e^{\nu/2}T = \text{constant}, \quad (5)$$
$$e^{\nu/2}(\mu + mc^2) = \text{constant}. \quad (6)$$

The cutoff condition comes from the energy conservation along a geodesic,

$$e^{\nu/2}(\epsilon + mc^2) = \text{constant}, \quad (7)$$

that leads to the cutoff (or *escape* energy) condition

$$(1 + W\beta) = e^{(\nu_b - \nu)/2}, \quad (8)$$

where $\nu_b \equiv \nu(r_b)$ the metric function at the boundary of the configuration, i.e. $W(r_b) = \epsilon_c(r_b) = 0$ (Merafina and Ruffini, 1989), and r_b is the boundary radius often called *tidal* radius. The above cutoff formula reduces to the known escape velocity condition $v_e^2 = -2\phi$ in the classical limit $c \to \infty$ ($e^{\nu/2} \approx 1 + \phi/c^2$) considered by King (1966), where $V = m\phi$ with ϕ the Newtonian gravitational potential, adopting the choice $V(r_b) = 0$.

The above conditions together with the Einstein equations lead to the system of equilibrium equations

$$\frac{d\hat{M}_{DM}}{d\hat{r}} = 4\pi\hat{r}^2\hat{\rho}, \quad (9)$$
$$\frac{d\theta}{d\hat{r}} = -\frac{1 - \beta_0(\theta - \theta_0)}{\beta_0}\frac{\hat{M}_{DM} + 4\pi\hat{P}\hat{r}^3}{\hat{r}^2(1 - 2\hat{M}_{DM}/\hat{r})}, \quad (10)$$
$$\frac{d\nu}{d\hat{r}} = \frac{2(\hat{M}_{DM} + 4\pi\hat{P}\hat{r}^3)}{\hat{r}^2(1 - 2\hat{M}_{DM}/\hat{r})}, \quad (11)$$
$$\beta(\hat{r}) = \beta_0 e^{\frac{\nu_0 - \nu(\hat{r})}{2}}, \quad (12)$$
$$W(\hat{r}) = W_0 + \theta(\hat{r}) - \theta_0\,. \quad (13)$$

In the limit $W \to \infty$ (i.e. $\epsilon_c \to \infty$) these system reduce to the equations considered in the original RAR model (Ruffini et al., 2015). We have introduced the same dimensionless quantities as in the original RAR model formulation: $\hat{r} = r/\chi$, $\hat{M}_{DM} = GM_{DM}/(c^2\chi)$, $\hat{\rho} = G\chi^2\rho/c^2$, $\hat{P} = G\chi^2P/c^4$, where $\chi = 2\pi^{3/2}(\hbar/mc)(m_p/m)$ and $m_p = \sqrt{\hbar c/G}$ the Planck mass. We note that the constants of the Tolman and Klein conditions are evaluated at the center $r = 0$, indicated with a subscript '0'.

We proceed now to discuss the initial and boundary conditions for the solution of the above system of equations (9–13), for given regular initial conditions at the center, $[M_{DM}(0) = 0, \theta(0) = \theta_0, \beta(0) = \beta_0, \nu(0) = 0, W(0) = W_0]$, for different DM particle mass m, to find a solution consistent with the DM halo observables of the Galaxy, which we give in next section. We show in figs. 1 and 2 the results of the numerical integration for the radial behaviour of the free RAR model parameters for a selected fermion mass $mc^2 = 48$ keV.

In fig. 1 we show the temperature parameter, β, as a function of the radial distance r, for a fermion mass $mc^2 = 48$ keV. We plot also the gravitational redshifted temperature $e^{\nu/2}\beta$, which is constant throughout the configuration, as requested by the thermodynamical equilibrium condition in section 2. For completeness, we show the gravitational potential, $e^{\nu/2}$, as a function of the radial distance r, from which it can be checked that the temperature is higher where the gravitational potential is deeper, as given by section 2.

Figure 2 shows the degeneracy parameter, θ, as a function of r, for a fermion mass $mc^2 = 48$ keV and for given halo boundary conditions taken from observations (see next section). It can be seen the three different regimes throughout the Galaxy: the degenerate quantum core (highly positive values of θ), the transition from positive to negative values where quantum corrections are still important and finally the region of highly negative values corresponding to a Boltzmannian regime.

For the same fermion mass, fig. 2 shows the cutoff parameter as a function of r. From this figure it can be clearly seen the boundary of the Galaxy introduced by the cutoff (se next section for details).

With the aid of the general features of the physical RAR model parameters shown in the above figures, we can see that the DM density distribution (see fig. 3 in section 3) shows in general a division of three physical regimes:

1. an inner core with radius r_c of almost constant density governed by quantum degeneracy (see the region of high positive values of the degeneracy parameter in fig. 2);
2. an intermediate region with a sharply decreasing density distribution followed by an extended plateau, where quantum corrections are still important (see the region of transition from positive to negative values of degeneracy in fig. 2); and
3. a Boltzmannian density tail (see highly negative values of the degeneracy parameter in fig. 2) showing a behavior $\rho \propto r^{-n}$ with $n > 2$ due to the cutoff constraint, as can be seen from fig. 2.

Indeed, the use of the quantum (fermionic) statistical treatment is justified in all the family of inner cores analyzed here for the Galaxy since they fulfill the condition $\lambda_B \gtrsim 3l_c$, where $l_c \sim n_c^{-1/3}$ is the interparticle mean distance within the core (with n_c the core particle density) and $\lambda_B = h/(2\pi mkT_c)^{1/2}$ the thermal de-Broglie wavelength at the core (see below in section 3 and also Ruffini et al., 2015).

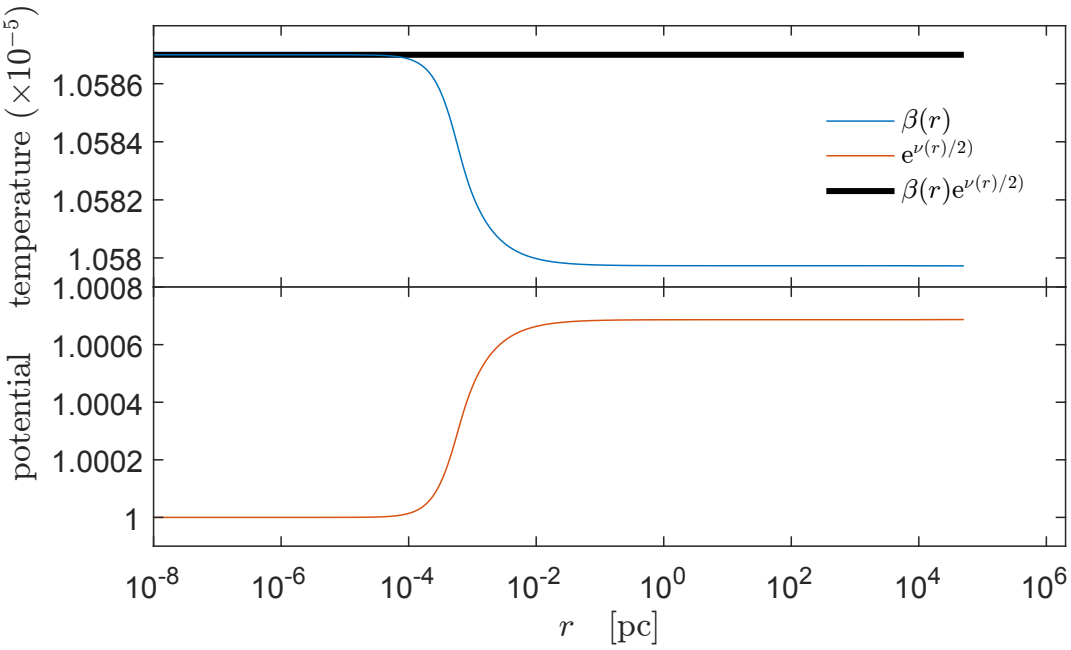

Figure 1: Upper panel: temperature parameter, β, as a function of the radial distance r, for a fermion mass mc^2 = 48 keV and for given halo boundary conditions taken from observations (see next section). We plot also the gravitational redshifted temperature $e^{\nu/2}\beta$ to check its constancy throughout the configuration as requested by the thermodynamical equilibrium condition (5). Lower panel: gravitational potential, $e^{\nu/2}$.

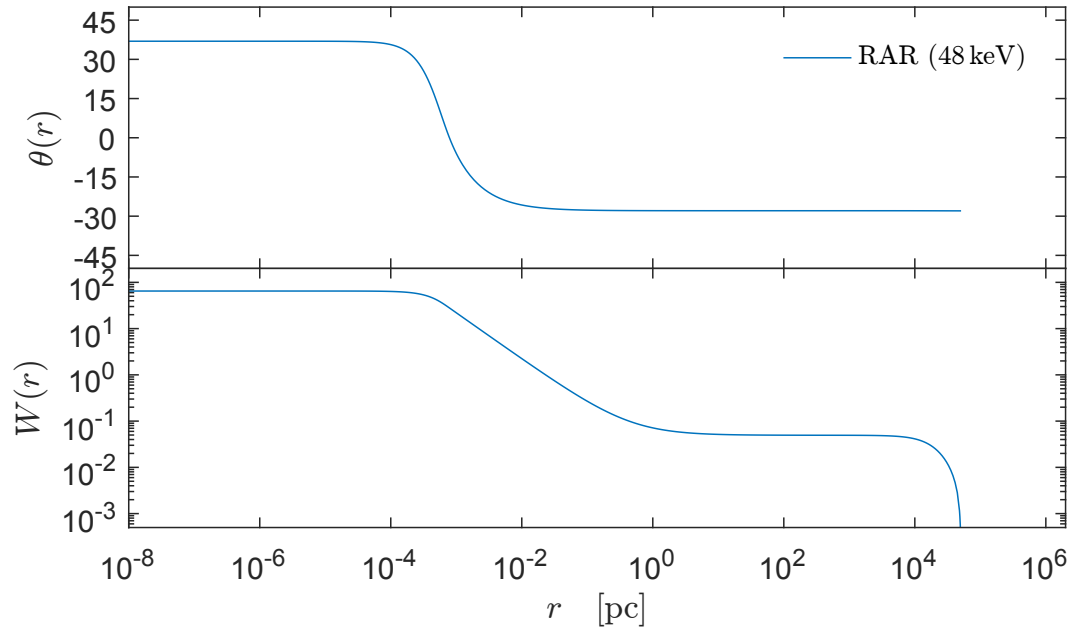

Figure 2: Upper panel: Degeneracy parameter, θ, as a function of the radial distance r, for a fermion mass mc^2 = 48 keV and for given halo boundary conditions taken from observations (see next section). It can be seen the three different regimes throughout the Galaxy: the degenerate quantum core (highly positive values of θ), the transition from positive to negative values where quantum corrections are still important and finally the region of highly negative values corresponding to a Boltzmannian regime. Lower panel: corresponding cutoff parameter, W.

The different regimes in the $\rho(r)$ profiles are also manifest in the DM rotation curve showing respectively (see fig. 4):

1. a linearly increasing circular velocity $v_{\rm DM} \propto r$ reaching a first maximum at the quantum core radius r_c;
2. a Keplerian $v_{\rm DM} \propto r^{-1/2}$ decreasing behavior representing the transition from quantum degeneracy to the dilute regime, continued again by a $v_{\rm DM} \propto r$ trend until reaching a second maximum at r_h, which we adopt as the one-halo scale length in our model;
3. a decreasing behavior consistent with the power law density tail $\rho \propto r^{-n}$ (with $n > 2$) due to the cutoff constraint.

The above more general *dense quantum core - classical halo* distribution appears as a consequence of the inclusion of finite temperature effects together with the possibility for the fermions to acquire positive values of the degeneracy parameter in the central regions of the equilibrium configurations (regardless of an eventual cutoff in the particle energy).

The fact that the fermions are immerse in an external gravitational field automatically leads to a radial gradient of the degeneracy leading to a highly degenerate and compact core at the center followed by a sharp transition to the more diluted and extended classical Boltzmann-like tail.

It is important to stress that our results markedly differ to the ones describing galactic halos solely by a highly-degenerate configuration or solely by a classical Boltzmann-like (or diluted Fermi-Dirac) one; see e.g. de Vega et al. (2014) and references therein. As we have shown both regimes exist inside the galaxy. Indeed, Randall et al. (2017) has recently shown in the specific case of dwarf galaxies that a fully degenerate self-gravitating system of fermions leads to rather compact halos in contrast with the observational values and that the problem is alleviated by the artificial addition of an isothermal density tail. Clearly, such a hybrid description is overcome by the unified core-halo description first presented in Ruffini et al. (2015) and generalized in this work.

It is interesting to recall that a similar core-halo structure obeying a Fermi-Dirac-like distribution function was shown to arise as the most probable final outcome (from a maximization entropy principle) of collisionless relaxation mechanisms (Lynden-Bell, 1967; Chavanis and Sommeria, 1998; Chavanis, 2004; Chavanis et al., 2015).

3. Application to the Milky Way

Based on the above morphological structure, we adopt as boundary conditions a DM halo mass with the observed value at two different radial locations in the Galaxy: a DM halo mass $M_{\rm DM}(r = 40\ {\rm kpc}) = 2 \times 10^{11} M_\odot$, consistent with the dynamics of the outer DM halo (see Gibbons et al., 2014, and also point (i) below), and $M_{\rm DM}(r = 12\ {\rm kpc}) = 5{\times}10^{10} M_\odot$, as constrained in Sofue (2013). Simultaneously, we require a quantum core of mass $M_{DM}(r = r_c) \equiv M_c = 4.2{\times}10^6 M_\odot$ enclosed *within* a radius $r_c = r_{p(S2)} = 6{\times}10^{-4}$ pc, the S2 star pericenter (Gillessen et al., 2009). This implies three boundary conditions for the three free RAR model central parameters, once the particle mass is given.

We consider here the extended high resolution rotation curve data of the Milky Way in Sofue (2013), ranging from pc scales up to $\sim 10^2$ kpc, together with the orbital data of the eight best resolved S-cluster stars taken from Gillessen et al. (2009). Our analysis will thus cover in total more than nine orders of magnitude of radial extent. According to Sofue (2013), the matter components of the Galaxy can be thus divided in 4 independent mass distributions laws, governed by different kinematics and dynamics:

i) the central ($10^{-3} \lesssim r \lesssim 2$) pc consisting in young S-stars and molecular gas, following a Keplerian law $v \propto r^{-1/2}$, and whose dynamics is dictated by a dark and compact object of mass $M_c \approx 4{\times}10^6 M_\odot$ centered in SgrA*;

ii) an intermediate spheroidal Bulge structure ($3 \lesssim r \lesssim 10^3$) pc composed mostly of older stars, and presenting a maximum bump in the velocity curve of $v \approx 250$ km/s at $r \sim 0.4$ kpc, with inner and main mass distributions explained by the exponential spheroid model

$$\rho(r) = \rho_c e^{-r/a_b}; \tag{14}$$

iii) an extended flat disk ($10^3 \lesssim r \lesssim 10^4$) pc including star forming regions, dust and gas, whose surface mass density is described by an exponential law

$$\Sigma(R) = \Sigma_0 e^{-R/a_d}, \qquad \Sigma_0 = M_d/(2\pi a_d^2), \tag{15}$$

being M_d the total disk mass (see Sofue, 2013 for the values of the central densities (ρ_c,Σ_0) and corresponding scale-lengths (a_b, a_d) of each baryonic (bulge+disk) model); and

iv) a spherical halo ($10^4 \lesssim r \lesssim 10^5$) pc dominated by DM and presenting a velocity peak of $v \approx 160$ km s^{-1} at about $r \sim 30$ kpc, followed by a decreasing density tail steeper than r^{-2}.

Following the standard assumption in the literature that baryonic and DM do not interact each other, we have calculated the total rotation curve as

$$v_{\rm rot} = \sqrt{r\frac{d\Phi_T}{dr}} = \sqrt{v_b^2(r) + v_d^2(r) + v_{\rm DM}^2(r)}, \tag{16}$$

where

$$\Phi_T = \Phi_b + \Phi_d + \Phi_{\rm DM}, \tag{17}$$

is the total gravitational potential generated by the sum of each component, and $v_b^2(r)$, $v_d^2(r)$ the baryonic squared circular velocities. We calculated the total (inner + main) bulge circular velocity using the same mass model parameters as in Sofue (2013). For the disk, we have performed the calculations with mass models parameters (M_d, r_d) slightly

changed with respect to those given in Sofue (2013), where the NFW DM profile was assumed. Such slight changes imply a shift in the disk velocity of up to 15% respect to the disk velocity model used in Sofue (2013), corresponding with a ~ 20 km/s maximum deviance. We do this change to improve the fit of the observational data when adopting our DM profile. Finally, $v^2_{\rm DM}(r)$ is the DM contribution computed numerically from the $M_{DM}(r)$ solution of (9–13), through the general relativistic formula for the velocity

$$v^2_{DM}(r) = \frac{GM_{DM}(r)}{r - 2GM_{DM}(r)/c^2}, \qquad (18)$$

according to the equations of motion of a test-particle in the spacetime metric (4).

We discuss in next the results of the numerical integration accounting for the full boundary condition problem in the case of the Milky Way within our model. The key result is that there is a continuous underlying DM distribution covering the whole observed Galactic extent, which not only governs the dynamics of the outer halo ($r \gtrsim$ 10 kpc), but also the central regions of the Galaxy ($r \lesssim$ 1 pc), while the intermediate region (1 pc $\lesssim r \lesssim$ 10 kpc) is dominated by the baryonic components (bulge+disk).

Figure 3 shows the RAR density profiles from 10^{-7} pc all the way to 10^5 pc, for three representative values of the fermion mass: 0.6 keV/c^2 (dotted yellow curve), 48 keV/c^2 (long-dashed gray curve) and 345 keV/c^2 (solid black curve). The dashed blue vertical lines indicate the position of the best resolved stars of the S-cluster (Gillessen et al., 2009). We show for the sake of comparison the NFW density profile as implemented in Sofue (2013) (dashed black curve). Generalized NFW profiles can be also used for a comparison with more recent results, considering these phenomenological profiles have been recently implemented and shown to increase the degree of compatibility with the Milky Way rotation curve (see e.g. Pato et al., 2015).

The Milky Way outermost DM halo behavior is subjected to the cutoff conditions: $W(r_b) \approx 0$ when $\rho(r_b) = 10^{-5} M_\odot/pc^3$, at the boundary radius $r_b = 50$ kpc (see fig. 3); with $\rho(r_b)$ the Local Group density as constrained in Sofue (2012). We note that the exact $W(r) = 0$ cutoff condition, is fulfilled in the limiting case $\rho(r) = 0$ achieved for $r \gtrsim r_b$. The limiting behavior of such a DM density profile is also consistent with a DM halo mass of $M_{\rm DM}(r = 40\ {\rm kpc}) = 2 \times 10^{11} M_\odot$ as required above, further implying a total Galactic mass (dark + baryonic) at r_b of $M_T(r_b) \approx 3 \times 10^{11} M_\odot$, of which 80% is DM according to our model (**i.e.** $M_{DM}(r_b) = 2.4 \times 10^{11} M_\odot$). It is clear that such a DM mass distribution must be also in agreement with the dynamical constraints set by the Galactic satellite dwarf observations, e.g. the Sagittarius (Sgr) dwarf satellite. Indeed, such observational constraints have been recently considered in Gibbons et al. (2014), who showed that their fulfillment requires a total mass of the Galaxy (at $\sim 80\%$ confidence level) $M_T(r \gtrsim 50\ {\rm kpc}) \approx 3 \times 10^{11} M_\odot$, in agreement with our results here. [1]

Figure 4 shows the RAR rotation curves in the same radial extent and for the same three representative values of the fermion mass in fig. 3. We show for the above three fermion masses the DM contribution to the total rotation curve, and, for the case of $mc^2 = 48$ keV, the total rotation curve (red thick curve) including the total baryonic (bulge + disk) component. From these three examples shown, it can be directly seen that only the RAR solutions with particle masses in the range $mc^2 = 48 - 345$ keV are in agreement with the Milky Way observables in the region $r \sim 10^{-3} - 10^5$ pc, where data are available. This is, the ones which are able to provide an alternative to the BH scenario in SgrA*. The blue star symbols represent the best resolved stars of the S-cluster (Gillessen et al., 2009) and their position in the plot has been evaluated as the *effective* circular velocity at pericenter, i.e. without considering the ellipticity of the orbits.

We further display in fig. 5 a zoom of fig. 4 (the most relevant curves) in the 1 – 35 kpc region and in linear scale. This allow us to better appreciate the difference between the diverse DM models in the radial window where the Rotation Curve is most relevant. Thus, fig. 5 compares the [baryon + DM] Rotation Curve fits against data, for the following DM models: (i) NFW as implemented in Sofue (2013) (continuous black); (ii) RAR models for $mc^2 = 48$ keV (solid red) and $mc^2 = 345$ keV (dashed green). We further plot in the same figure the DM-only contribution to the corresponding total Rotation Curve for each DM model.

As already evidenced in fig. 4, and due to the specific MW halo boundary conditions imposed to all the RAR solutions worked out in this paper (see above), there is an almost perfect match (within 1%) in all RAR curves from inner-halo scales and beyond (i.e within the increasing trend $v_{DM} \propto r$ and up to r_b). In particular, the coinciding behaviour between the two ($mc^2 = 48, 345$ keV) different DM RAR profiles in the zoomed-in region, together with the addition of the unchanged baryonic contributions, explains the coinciding total (baryon + RAR-DM) Rotation Curve fits (solid red and dashed green).

Instead, there is a visible and appreciable difference when comparing between the (intrinsically) distinct RAR and NFW (DM-only) models, mainly in the region of 1 – 10 kpc. Nevertheless, and regardless of this discrepancy, both profiles provide a comparably good fit to the total Rotation Curve, given the baryonic physics (bulge + disk)

[1] Constraints on the total (virial) Galaxy mass from the Sgr dwarf stream (Belokurov et al., 2014) may imply even larger values of $M_T(r = 100\ {\rm kpc}) \approx 4 \times 10^{11} M_\odot$ (Gibbons et al., 2014). Nevertheless, this stream motion of tidally disrupted stars is likely related with merging processes that date back to the DM halo formation of the Galaxy (Lynden-Bell and Lynden-Bell, 1995), while our modeling does not include mergers, nor dynamical DM accretion from environment, which may likely increase the Galaxy mass during its whole evolution.

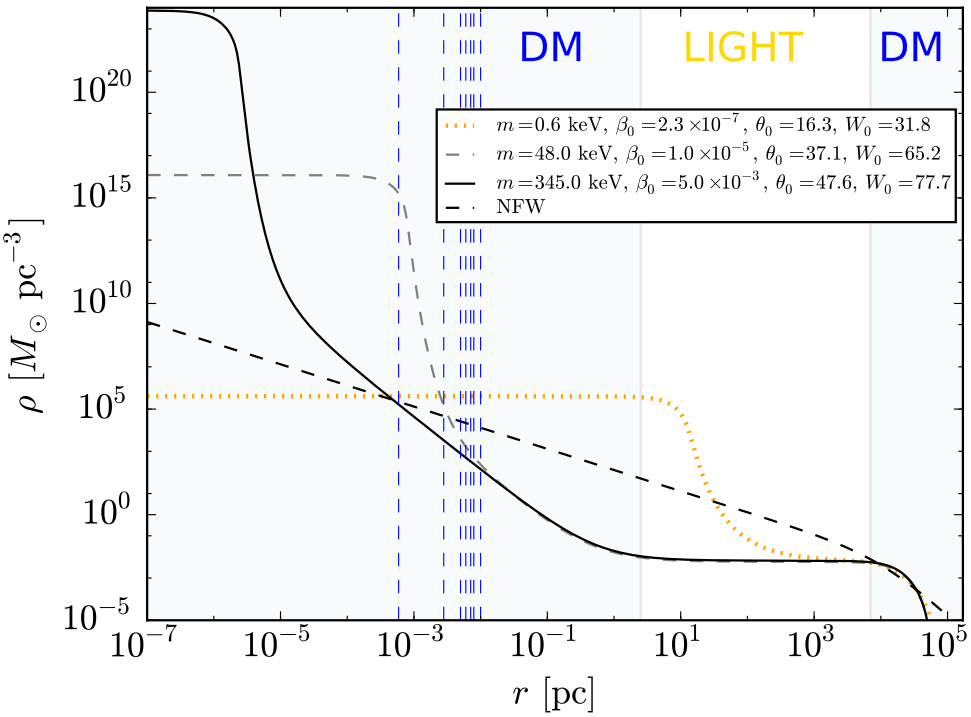

Figure 3: (Color online) Theoretical density profiles from 10^{-7} pc all the way to 10^5 pc, for three representative fermion masses in the mc^2 ~keV region: 0.6 keV (dotted yellow curve), 48 keV (long-dashed gray curve) and 345 keV (solid black curve). The dashed blue lines indicate the position of the S-cluster stars (Gillessen et al., 2009). We show for the sake of comparison the NFW density profile as obtained in Sofue (2013) (dashed black curve). See the text for additional details.

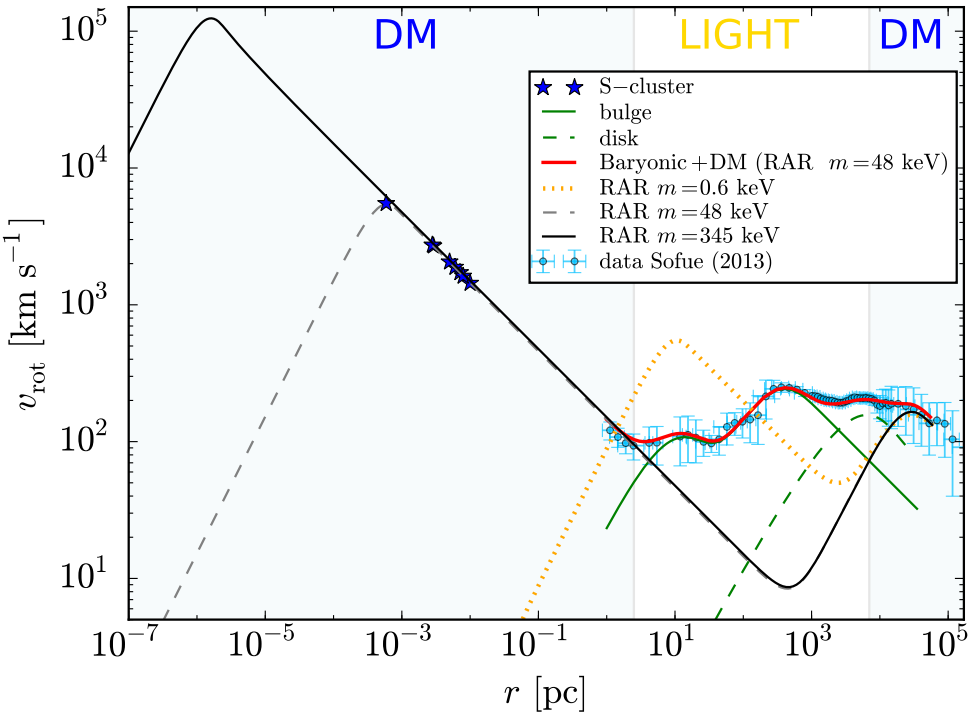

Figure 4: (Color online) Theoretical RAR rotation curves from 10^{-7} pc all the way to 10^5 pc, for three representative fermion masses in the mc^2 ~keV region: 0.6 keV (dotted yellow curve), 48 keV (long-dashed gray curve) and 345 keV (solid black curve). These RAR solutions are in agreement with all the Milky Way observables from $\sim 10^{-3}$ pc to $\sim 10^5$ pc. For the case of $mc^2 = 48$ keV, we include the total rotation curve (red thick curve) including the total baryonic (bulge + disk) component. The star symbols represent the eight best resolved S-cluster stars (Gillessen et al., 2009). See the text for additional details.

is the one which dominate at those scales. While the slight exceeding trend in total v_{rot} of [baryon + NFW-DM] (black curve) respect to [baryon + RAR-DM] (e.g. red curve)[2] is explained by the cuspiness of the NFW (inner-halo) density profile respect to the cored RAR profile at those scales. At outer radii, $r > 10$ kpc, DM dominates over baryons, and now the exceeding trend in v_{rot} of [baryon + RAR-DM] over [baryon + NFW-DM] is directly explained by the difference in the power-law behaviours of NFW ($\rho \propto r^{-3}$), respect to RAR ($\rho \propto r^{-n}$), with $n > 2$.

Finally, it is important to stress that we have just applied a plain fitting procedure to the data (i.e. two fixed halo boundary conditions for DM RAR equations, with given simple baryonic models taken from literature), and that the only outcome of applying any more sophisticated statistical method (such as a Monte Carlo Markov Chain, or similar) is of a further improvement of our fittings.

We summarize as follows the more general results worked out in this paper, including the examples shown in the figures below:

1. The fermion mass range $mc^2 \lesssim 10$ keV is firmly ruled out by the present analysis because the corresponding rotation curve starts to exceed the total velocity observed in the baryonic (bulge) dominated region $r \approx 2 - 100$ pc (including upper bound in error bars; see for example the highly exceeding case of $mc^2 \sim 1$ keV (dotted yellow curve) in fig. 4). For these particle masses the DM distribution produces a large overshoot over the observed inner-rotation curve. This implies that our lower limit to the fermion mass will hold also for different and more accurate inner-baryonic models (e.g. Portail et al., 2017) which, in any case, change the total inner-rotation curve only by a small percentage with respect to the one we have used in this work. In addition, for these relatively low particle masses below 10 keV, and due to the overshooting in the inner-bulge velocity region, it is clear that these solutions only fulfill with the chosen halo boundary conditions and do not provide an alternative to the central BH in SgrA*.
2. All RAR model solutions for a fermion mass in the range $mc^2 \approx 10 - 345$ keV give a nearly equal total rotation curve (as the red thick curve shown in fig. 4 for the case of $mc^2 = 48$ keV) in the aforementioned baryonic dominated region above ~ 2 pc, since the DM potential there produces a negligible contribution with respect to the baryonic one (see also point 9 below).
3. In the intermediate fermion mass range $mc^2 = 10 - 48$ keV, the theoretical rotation curve is not in conflict with any of the observed data and DM inferences in Sofue (2013), but the compactness of the quantum core is not enough to be an alternative to the central BH scenario in SgrA*.
4. For fermion masses $mc^2 = 48 - 345$ keV, the RAR solutions with corresponding initial parameters (β_0, θ_0, W_0) explain the Galactic DM halo and, provide at the same time, an alternative for the central BH scenario. The mass lower bound in m is imposed by the dynamics of the stellar S-cluster. Namely, the quantum core radius of the solutions for $mc^2 \geq 48$ keV are always smaller or equal than the radius of the S-2 star pericenter, i.e. $r_c \leq r_{p(S2)} = 6 \times 10^{-4}$ pc $\approx 1.5 \times 10^3 r_{\rm Sch}$.
5. There is a mass upper bound of $mc^2 = 345$ keV that corresponds to the last stable configuration before reaching the critical mass for gravitational collapse ($M_c^{cr} \propto m_{\rm Planck}^3/m^2$), and calculated following the turning point criterion for core-collapse in Argüelles and Ruffini, 2014. The core radius of the critical configuration is $r_c \approx 4\, r_{\rm Sch}$, with $r_{\rm Sch}$ the Schwarzschild radius of a $4.2 \times 10^6 M_\odot$ BH (see also Argüelles et al., 2014b). In particular the following set of initial conditions

$$[\beta_0 = 1.03 \times 10^{-5}, \theta_0 = 37.14, W_0 = 65.252],$$

$$[\beta_0^{cr} = 5.04 \times 10^{-3}, \theta_0^{cr} = 47.59, W_0^{cr} = 77.706],$$

   were obtained for the lower and upper DM particle mass bounds respectively (the upper index 'cr' stands for the critical configuration).
6. For a relatively low compact core as the one calculated for $mc^2 = 10.4$ keV, we have $\lambda_B = 3.1\, l_c$; while in the most compact one (black solid curve in fig. 3 for $mc^2 = 345$ keV) we have $\lambda_B = 4.0\, l_c$. This justifies our use of the quantum fermion statistical treatment.
7. The DM contribution to the Galactic halo rotation curves becomes necessary above ~ 7 kpc (see figs. 4 and 5). This is in agreement with the DM model-independent observational analysis by Iocco et al. (2015).
8. Interestingly, in the mass range $mc^2 = 10 - 345$ keV the RAR DM distribution predicts Keplerian rotation curves at $r \lesssim 2$ pc (see fig. 4). This feature is in agreement with the apparent Keplerian trend observed in the innermost gas data points in Sofue (2013), with the caveat that the tracers in the region $1 - 100$ pc might not follow the gravitational potential due to the more complex bar pattern speed present in the Milky Way central region (see also the discussion section in Sofue (2013)).
9. In the above mass range the full rotation curve $v_{\rm rot} = \sqrt{r(d\Phi_T/dr)}$ (see solid red line in fig. 4) is in good agreement with observations within the observational errors. In addition, the minimum in the DM rotation curve *coincides* with the absolute maximum of $v_{\rm rot}$ (i.e. the bulge peak) attained at $r \approx 0.4$ kpc. This

[2] Slight changes in the disk parameters where applied within RAR model-fitting respect to those given in Sofue (2013) where NFW was applied, as explicited above in this section.

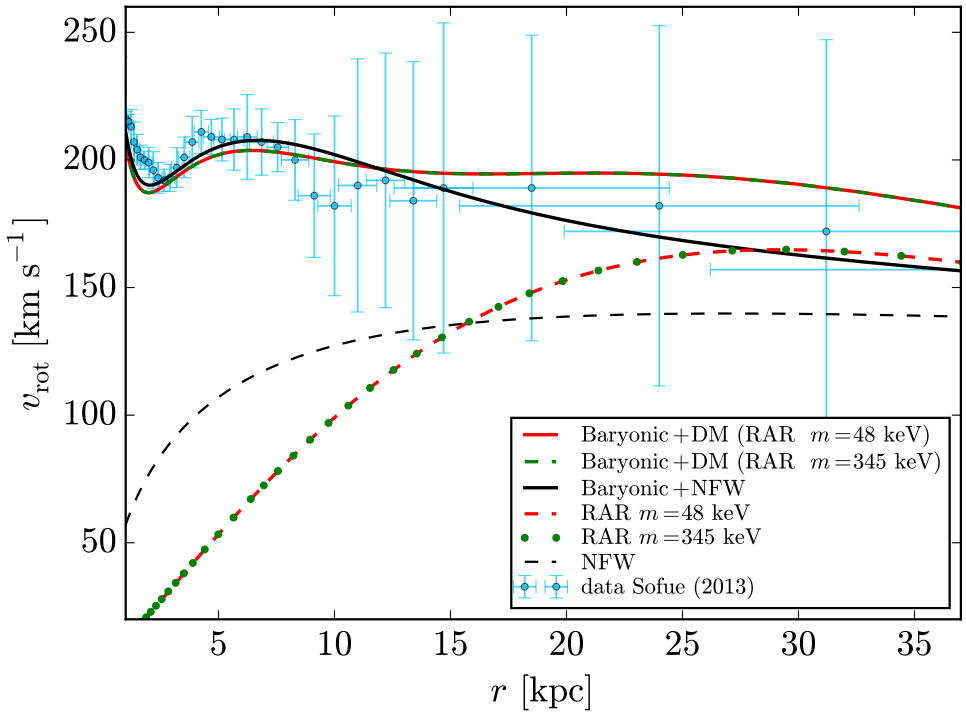

Figure 5: (Color online) Comparison of the total (DM plus baryonic) rotation curves as given by the RAR model (for a fermion mass mc^2 = 48 keV and 345 keV) and the phenomenological NFW model (from Sofue (2013), but see also Pato et al. (2015) for the possible implementation of generalized NFW models) in the region r = 1 – 35 kpc. Within the region 1 – several kpc, the contribution of the baryonic components dominates respect to the DM, while at distances $r \gtrsim 10$ kpc there is, instead, an increasing dominance of the DM component (see text for further details).

peculiar fact might provide a clue for a deeper understanding of the complex ensemble history of the baryonic stellar bulge on top of the previously formed DM structure. This inference, as the previous one, relies on the assumption that the tracers in such a Galaxy region follow the gravitational potential, and therefore such a link must be taken with caution considering the lack of axisimmetry of the potential at those bulge scales (see however Sofue (2013) where such effects were further discussed).

4. Concluding remarks

It is now clear from our results that gravitationally bounded systems based on fermionic phase-space distributions including a particle energy cutoff (or escape velocity effects) and central degeneracy, can explain the DM content in the Galaxy while providing a natural alternative for the central BH scenario in SgrA*.

Specifically, we have shown that:

- fermion masses $mc^2 \lesssim 10$ keV are ruled out by the Milky Way rotation curve since the contribution of the DM to the rotation curve highly exceeds the observed values (see fig. 4 in section 3);
- for mc^2 = 48 – 345 keV, the DM halo distribution is in agreement with standard data of the Milky Way rotation curve tracers, and harbors a dense quantum core of $4 \times 10^6 M_\odot$ within the S2-star pericenter;
- for mc^2 = 10 – 48 keV the DM distribution is also in agreement with the Galaxy rotation curve data but the compactness of the DM quantum core is not enough to explain the S-cluster dynamics and so to be an alternative to the central BH scenario.

Our general results on the DM distribution in galaxies can be considered as complementary to those based on standard cosmological simulations. However, the latter being based on N-body purely Newtonian simulations, contrast with our semi-analytical four-parametric approach which has the chance to include more rich physical ingredients, such as quantum statistics (arising from specific phase-space relaxation mechanisms), thermodynamics, and gravity.

An important aspect of the particle mass range of few 10 – 100 keV obtained here from galactic observables, is that it produces basically the same behavior in the power spectrum (down to Mpc scales) from that of standard ΛCDM cosmologies, thus providing the expected large-scale structure (see Boyarsky et al., 2009a, for details). In addition, it is not 'too warm' (i.e. our masses are larger than $mc^2 \sim 1 - 3$ keV) to enter in tension with current Lyα forest constraints (Boyarsky et al., 2009b; Viel et al., 2013) and the number of Milky Way satellites (Tollerud et al., 2008), as in standard ΛWDM cosmologies.

Our model naturally provides cored inner DM halos (our fermionic phase-space distributions imply an extended plateau in the DM density profile on halo scales in a way that they resemble Burkert or cored Einasto profiles (Ruffini et al., 2015)), without developing undesired cuspy density trends on such scales as the ones found in N-body simulations (Navarro et al., 1997). Such a marked difference between both kind of density profiles, the cored (RAR) and cuspy (NFW), arises due to the physics involved in the two different approaches, which in turn may provide an important insight to one of the main open problems in standard ΛCDM cosmology, i.e. the so-called core-cusp problem (de Blok, 2010).

Interestingly, in Walker and Peñarrubia (2011) it has been provided a clear observational evidence for the cored nature (DM model independent) of the DM density profiles in dwarf spheroidal galaxies such as Sculptor. We show in an accompanying article (Argüelles, et al. 2018; to be submitted) that these DM halo features, i.e. the constant inner halo density and halo scale-radius, are in agreement with the RAR model results applied to dwarf galaxies.

Moreover, in the accompanying article (Argüelles, et al. 2018; to be submitted), we show that a key point of the present RAR model is the ability to predict entire DM halo configurations which fulfills the observed universal properties of galaxies, such as the *central BH mass - total halo mass* ($M_{\rm BH}$-$M_{\rm tot}$) and the surface DM halo density relation ($\Sigma_{0D} \approx$ constant), for a unique DM fermionic mass. At the same time, it provides, on astrophysical basis, possible clues on the formation of supermassive BHs in galactic nuclei.

All the above offer significant support for our keV-scale fermions as DM, which may well co-exist harmonically with other DM species in the universe. These aspects will have to interplay with the physics of elementary particles regarding the nature of these fermions: Majorana neutrinos, supersymmetric particles, sterile neutrinos, etc.; as well as with the possible detection through decaying processes involving weak interactions. Indeed, DM fermion masses within the relatively narrow window obtained here, $mc^2 = 48 - 345$ keV, have also arisen within different microscopic models based on extensions of the standard model, and consistent with all cosmological, large scale structure, and X-ray constraints, as the ones considered in Boyarsky et al. (2009b); Patwardhan et al. (2015).

Acknowledgments

We thank the referee for the very constructive and clear suggestions. A.K. is supported by the Erasmus Mundus Joint Doctorate Program by Grants Number 2014–0707 from the agency EACEA of the European Commission.

References

R. W. Michie, On the distribution of high energy stars in spherical stellar systems, MNRAS 125 (1963) 127.

I. R. King, The structure of star clusters. III. Some simple dynamical models, AJ 71 (1966) 64, doi:10.1086/109857.

D. Lynden-Bell, Statistical mechanics of violent relaxation in stellar systems, MNRAS 136 (1967) 101.

J. Binney, S. Tremaine, Galactic Dynamics: Second Edition, Princeton University Press, 2008.

R. Ruffini, S. Bonazzola, Systems of Self-Gravitating Particles in General Relativity and the Concept of an Equation of State, Physical Review 187 (1969) 1767–1783, doi:10.1103/PhysRev.187.1767.

M. R. Baldeschi, G. B. Gelmini, R. Ruffini, On massive fermions and bosons in galactic halos, Physics Letters B 122 (1983) 221–224, doi:10.1016/0370-2693(83)90688-3.

L. Hui, J. P. Ostriker, S. Tremaine, E. Witten, Ultralight scalars as cosmological dark matter, Phys. Rev. D 95 (4) 043541, doi:10.1103/PhysRevD.95.043541.

J. G. Gao, M. Merafina, R. Ruffini, The semidegenerate configurations of a selfgravitating system of fermions, A&A 235 (1990) 1–7.

R. Ruffini, L. Stella, On semi-degenerate equilibrium configurations of a collisionless self-gravitating Fermi gas, A&A 119 (1983) 35–41.

M. Merafina, R. Ruffini, Systems of selfgravitating classical particles with a cutoff in their distribution function, A&A 221 (1989) 4–19.

G. Ingrosso, M. Merafina, R. Ruffini, F. Strafella, System of self-gravitating semidegenerate fermions with a cutoff of energy and angular momentum in their distribution function, A&A 258 (1992) 223–233.

P.-H. Chavanis, Generalized thermodynamics and kinetic equations: Boltzmann, Landau, Kramers and Smoluchowski, Physica A Statistical Mechanics and its Applications 332 (2004) 89–122, doi:10.1016/j.physa.2003.09.061.

C. Argüelles, I. Siutsou, R. Ruffini, J. Rueda, B. Machado, On the core-halo constituents of a semi-degenerate gas of massive fermions, in: Probes of Dark Matter on Galaxy Scales, 30204, 2013.

H. J. de Vega, P. Salucci, N. G. Sanchez, Observational rotation curves and density profiles versus the Thomas-Fermi galaxy structure theory, MNRAS 442 (2014) 2717–2727, doi:10.1093/mnras/stu972.

C. R. Argüelles, R. Ruffini, I. Siutsou, B. Fraga, On the distribution of dark matter in galaxies: Quantum treatments, Journal of Korean Physical Society 65 (2014a) 801–804, doi:10.3938/jkps.65.801.

I. Siutsou, C. R. Argüelles, R. Ruffini, Dark matter massive fermions and Einasto profiles in galactic haloes, Astronomy Reports 59 (2015) 656–666, doi:10.1134/S1063772915070124.

R. Ruffini, C. R. Argüelles, J. A. Rueda, On the core-halo distribution of dark matter in galaxies, MNRAS 451 (2015) 622–628, doi:10.1093/mnras/stv1016.

P.-H. Chavanis, M. Lemou, F. Méhats, Models of dark matter halos based on statistical mechanics: The fermionic King model, Phys. Rev. D 92 (12) 123527, doi:10.1103/PhysRevD.92.123527.

N. Bilic, F. Munyaneza, G. B. Tupper, R. D. Viollier, The dynamics of stars near Sgr A* and dark matter at the center and in the halo of the galaxy, Progress in Particle and Nuclear Physics 48 (2002) 291–300, doi:10.1016/S0146-6410(02)00136-9.

Y. Sofue, Rotation Curve and Mass Distribution in the Galactic Center - From Black Hole to Entire Galaxy, PASJ 65 (2013) 118, doi:10.1093/pasj/65.6.118.

S. Gillessen, F. Eisenhauer, T. K. Fritz, H. Bartko, K. Dodds-Eden, O. Pfuhl, T. Ott, R. Genzel, The Orbit of the Star S2 Around SGR A* from Very Large Telescope and Keck Data, ApJ 707 (2009) L114–L117, doi:10.1088/0004-637X/707/2/L114.

R. Ruffini, C. R. Argüelles, B. M. O. Fraga, A. Geralico, H. Quevedo, J. A. Rueda, I. Siutsou, Black Holes in Gamma Ray Bursts and Galactic Nuclei, International Journal of Modern Physics D 22 1360008, doi:10.1142/S0218271813600080.

R. C. Tolman, On the Weight of Heat and Thermal Equilibrium in General Relativity, Physical Review 35 (1930) 904–924, doi:10.1103/PhysRev.35.904.

O. Klein, On the Thermodynamical Equilibrium of Fluids in Gravitational Fields, Reviews of Modern Physics 21 (1949) 531–533, doi:10.1103/RevModPhys.21.531.
L. Randall, J. Scholtz, J. Unwin, Cores in Dwarf Galaxies from Fermi Repulsion, MNRAS 467 (2017) 1515–1525, doi:10.1093/mnras/stx161.
P.-H. Chavanis, J. Sommeria, Degenerate equilibrium states of collisionless stellar systems, MNRAS 296 (1998) 569–578, doi:10.1046/j.1365-8711.1998.01414.x.
S. L. J. Gibbons, V. Belokurov, N. W. Evans, 'Skinny Milky Way please', says Sagittarius, MNRAS 445 (2014) 3788–3802, doi:10.1093/mnras/stu1986.
M. Pato, F. Iocco, G. Bertone, Dynamical constraints on the dark matter distribution in the Milky Way, J. Cosmology Astropart. Phys. 12 001, doi:10.1088/1475-7516/2015/12/001.
Y. Sofue, Grand Rotation Curve and Dark Matter Halo in the Milky Way Galaxy, PASJ 64, doi:10.1093/pasj/64.4.75.
V. Belokurov, S. E. Koposov, N. W. Evans, J. Peñarrubia, M. J. Irwin, M. C. Smith, G. F. Lewis, M. Gieles, M. I. Wilkinson, G. Gilmore, E. W. Olszewski, M. Niederste-Ostholt, Precession of the Sagittarius stream, MNRAS 437 (2014) 116–131, doi:10.1093/mnras/stt1862.
D. Lynden-Bell, R. M. Lynden-Bell, Ghostly streams from the formation of the Galaxy's halo, MNRAS 275 (1995) 429–442, doi:10.1093/mnras/275.2.429.
M. Portail, O. Gerhard, C. Wegg, M. Ness, Dynamical modelling of the galactic bulge and bar: the Milky Way's pattern speed, stellar and dark matter mass distribution, MNRAS 465 (2017) 1621–1644, doi:10.1093/mnras/stw2819.
C. R. Argüelles, R. Ruffini, Are the most super-massive dark compact objects harbored at the center of dark matter halos?, International Journal of Modern Physics D 23 1442020, doi:10.1142/S0218271814420206.
C. R. Argüelles, R. Ruffini, B. M. O. Fraga, Critical configurations for a system of semidegenerate fermions, Journal of Korean Physical Society 65 (2014b) 809–813, doi:10.3938/jkps.65.809.
F. Iocco, M. Pato, G. Bertone, Evidence for dark matter in the inner Milky Way, Nature Physics 11 (2015) 245–248, doi:10.1038/nphys3237.
A. Boyarsky, O. Ruchayskiy, M. Shaposhnikov, The Role of Sterile Neutrinos in Cosmology and Astrophysics, Annual Review of Nuclear and Particle Science 59 (2009a) 191–214, doi:10.1146/annurev.nucl.010909.083654.
A. Boyarsky, J. Lesgourgues, O. Ruchayskiy, M. Viel, Realistic Sterile Neutrino Dark Matter with KeV Mass does not Contradict Cosmological Bounds, Physical Review Letters 102 (20) 201304, doi:10.1103/PhysRevLett.102.201304.
M. Viel, G. D. Becker, J. S. Bolton, M. G. Haehnelt, Warm dark matter as a solution to the small scale crisis: New constraints from high redshift Lyman-α forest data, Phys. Rev. D 88 (4) 043502, doi:10.1103/PhysRevD.88.043502.
E. J. Tollerud, J. S. Bullock, L. E. Strigari, B. Willman, Hundreds of Milky Way Satellites? Luminosity Bias in the Satellite Luminosity Function, ApJ 688 277-289, doi:10.1086/592102.
J. F. Navarro, C. S. Frenk, S. D. M. White, A Universal Density Profile from Hierarchical Clustering, ApJ 490 (1997) 493–508.
W. J. G. de Blok, The Core-Cusp Problem, Advances in Astronomy 2010 789293, doi:10.1155/2010/789293.
M. G. Walker, J. Peñarrubia, A Method for Measuring (Slopes of) the Mass Profiles of Dwarf Spheroidal Galaxies, ApJ 742 20, doi:10.1088/0004-637X/742/1/20.
A. V. Patwardhan, G. M. Fuller, C. T. Kishimoto, A. Kusenko, Diluted equilibrium sterile neutrino dark matter, Phys. Rev. D 92 (10) 103509, doi:10.1103/PhysRevD.92.103509.